PALEONTOLOGY

Developmental biology of *Helicoforamina* reveals holozoan affinity, cryptic diversity, and adaptation to heterogeneous environments in the early Ediacaran Weng'an biota (Doushantuo Formation, South China)

Zongjun Yin[1,2]*, Weichen Sun[1,2,3], Pengju Liu[4], Maoyan Zhu[1,2,5], Philip C. J. Donoghue[6]*

The exceptional fossil preservation of the early Ediacaran Weng'an biota provides a unique window on the interval of Earth history in which animal lineages emerged. It preserves a diversity of similarly ornamented encysted developmental stages previously interpreted as different developmental stages of one taxon. Although *Helicoforamina wenganica* is distinguished from other forms by a helical groove or canal, it has been interpreted as a developmental stage of cooccurring metazoan, nonmetazoan holozoan, or green algal taxa. Using x-ray microtomography, we show that *Helicoforamina* developed through one-, four-, and eight-cell stages, to hundreds and thousands of cells. Putative hatchlings are artifacts of incompletely preserved cyst walls. Our results preclude inclusion of *Helicoforamina* into life cycles assembled from other components of the Weng'an biota but support a holozoan affinity. The similarly ornamented encysted forms shared among the diverse Weng'an biota represent parallel adaptations to the temporally and spatially heterogeneous Ediacaran shallow marine environments.

INTRODUCTION

The early Ediacaran Weng'an biota of the Doushantuo Formation (609 million years old, Weng'an County, Guizhou Province, Southwest China) is one of the few windows of exceptional preservation at the time in Earth history in which molecular clock analyses estimate the fundamental clades and body plans of animal to have emerged (*1*, *2*). The biota is dominated by a diversity of developmental stages of microscopic organisms preserved with high fidelity, including not only component cells but also subcellular organelles and cytoplasmic structures (*3*). Hence, the Weng'an biota affords a uniquely direct insight into the developmental evolution of early body plans. However, interpretation of the fossils has proven challenging because the component developmental stages lack the systematically distinctive features of body plans and because of the difficulty of disambiguating developmental stages of the same organism from developmental stages of disparate organisms (*4*–*6*). This is no more obvious than for the enigmatic *Helicoforamina*, which has variously been interpreted to represent nonmetazoan holozoans [holozoans include ichthyosporeans, filastereans, choanoflagellates, and metazoans (*4*)], green algae (*7*), or, most commonly, as the long-sought late embryonic stages of metazoans otherwise represented by *Megasphaera* (*8*).

Helicoforamina is part of a broader complex of embryo-like fossils that includes *Tianzhushania*, *Megasphaera*, *Caveasphaera*, and *Spiralicellula* (Fig. 1). *Megasphaera* is known from developmental stages representative of successive rounds of equal palintomy (*9*, *10*), generally considered a senior synonym of *Parapandorina* (several to tens of cell stages) *and Megaclonophycus* (hundreds of cell stages) (*11*). *Megasphaera ornata* is distinguished in preserving an outer envelope with a cerebral, fractal, or dimpled surface ornamentation (Fig. 1, A to C) (*10*), but its distinction from other genera has been considered taphonomic rather than taxonomic (*12*). A similar envelope is encountered in co-occurring *Spiralicellula* (*7*) and *Caveasphaera* (*13*), but *Spiralicellula* is distinguished by its spiral cell morphology (Fig. 1, D and E) and *Caveasphaera* exhibits a different embryology of branching cell masses (Fig. 1, F to H) and shows no evidence of binary reductive palintomy (*13*). Co-occurring *Helicoforamina wengica* (Fig. 1, I to M) is of comparable size (500- to 900-μm diameter, mean = 748.7 μm, n = 314, SD = 94.3) to *Megasphaera* and has an envelope that is effectively indistinguishable from that of *Megasphaera* except for the presence of a dextrally coiled helical canal, groove, and/or sequence of pores that have been interpreted as a developing excystment structure, sites of cilia, or gas exchange (*8*). This helical structure is limited to the multilayered surface envelope (Fig. 1, I to T), completing three dextral loops in its course from one pole of the envelope to the other. However, the morphology of some specimens has been interpreted as evidence of uncoiling and invagination, such that the helical structure is imposed on natural internal molds of the envelope (*8*).

In its first detailed description, Xiao *et al.* (*8*) entertained two interpretations; one, which was later adopted by Huldtgren *et al.* (*4*), posited that *Helicoforamina* represented a one-cell egg that developed into the multicelled *Spiralicellula* (Fig. 2A), which is composed of cells that are similarly dextrally spiraled. This was effectively dismissed on the observation that the spirals in *Spiralicellula* complete only two loops of the cell (Fig. 1, D and E), do not always extend between poles, and there is no evidence for the transformation of the inner body of *Helicoforamina* and the multiple helical cells of *Spiralicellula*. In their preferred hypothesis, Xiao *et al.* (*8*) interpreted *Helicoforamina* as the postblastula developmental product of *Megasphaera* that, in turn, developed into *Sinocyclocyclicus*, a co-occurring tubular body fossil interpreted as a cnidarian (Fig. 2B) (*14*, *15*). If correct, they argued that intermediate forms would be discovered demonstrating the reorganization of *Megaclonophycus*-stage

[1]State Key Laboratory of Palaeobiology and Stratigraphy, Nanjing Institute of Geology and Palaeontology, Chinese Academy of Sciences, Nanjing 210008, China. [2]CAS Center for Excellence in Life and Paleoenvironment, Nanjing 210008, China. [3]University of Science and Technology of China, Hefei 230026, China. [4]Institute of Geology, Chinese Academy of Geological Sciences, Beijing 100037, China. [5]College of Earth and Planetary Sciences, University of Chinese Academy of Sciences, Beijing 100049, China. [6]School of Earth Sciences, University of Bristol, Life Sciences Building, Tyndall Avenue, Bristol BS8 1TQ, UK.
*Corresponding author. Email: zjyin@nigpas.ac.cn (Z.Y.); phil.donoghue@bristol.ac.uk (P.C.J.D.)

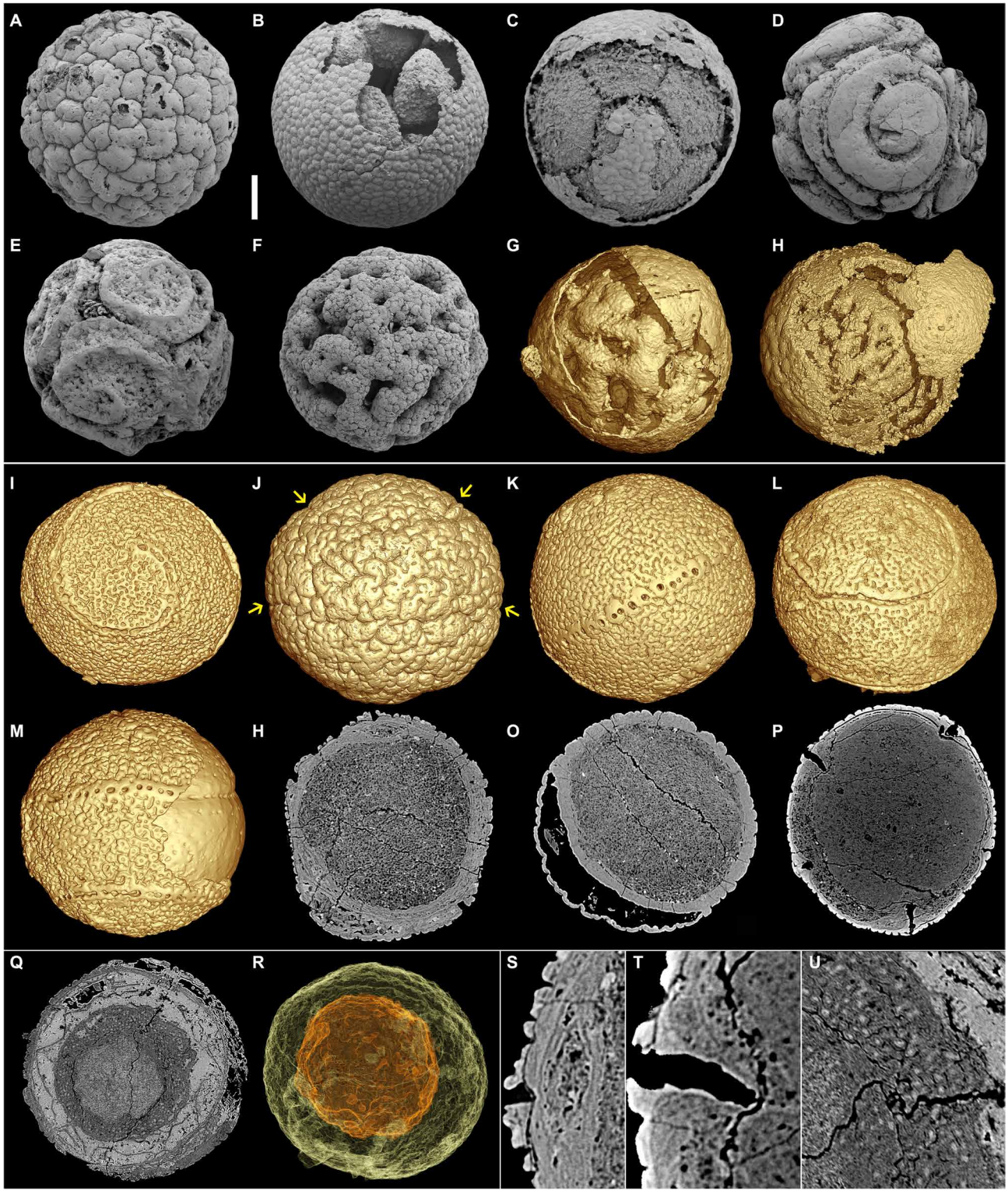

Fig. 1. Encysted embryo-like fossils with similar ornamentation from the Weng'an biota. (**A** to **C**) *Megasphaera*, scanning electron microscopy (SEM) images (*43*). (A) NIGP127672. (B) NIGP127673. (C) NIGP127674. (**D** and **E**) *Spiralicellula*, SEM images. (D) NIGP127675. (E) NIGP127676. (**F** to **H**) *Caveasphaera* (*13*). (**F**) SEM image, NIGP171728. (**G** and **H**) Surface renderings. (G) NIGP171725. (H) NIGP171726. (**I** to **M**) *Helicoforamina*, surface renderings. (I) NIGP173059. (J) NIGP173060. (K) NIGP173061. (L) NIGP173062. (M) NIGP173063. (**N** to **Q**) Virtual sections of (I) to (L), respectively. (**R**) Transparent models of (L), showing shrunken internal body. (**S** and **T**) Magnifications of (N) and (P), respectively, showing the detail of the histology of the envelopes at the spots where the helical canals and pores developed. (**U**) Magnification of (Q), showing putative subcellular structures within the internal body. Scale bars, (A) 154 μm, (B) 134 μm, (C) 150 μm, (D) 190 μm, (E) 210 μm, (F) 87 μm, (G) 118 μm, (H) 168 μm, (I) 137 μm, (J and O) 140 μm, (K) 132 μm, (M) 150 μm, (L, Q, and R) 114 μm, (N) 135 μm, (P) 147 μm, (S) 45 μm, (T) 33 μm, and (U) 30 μm.

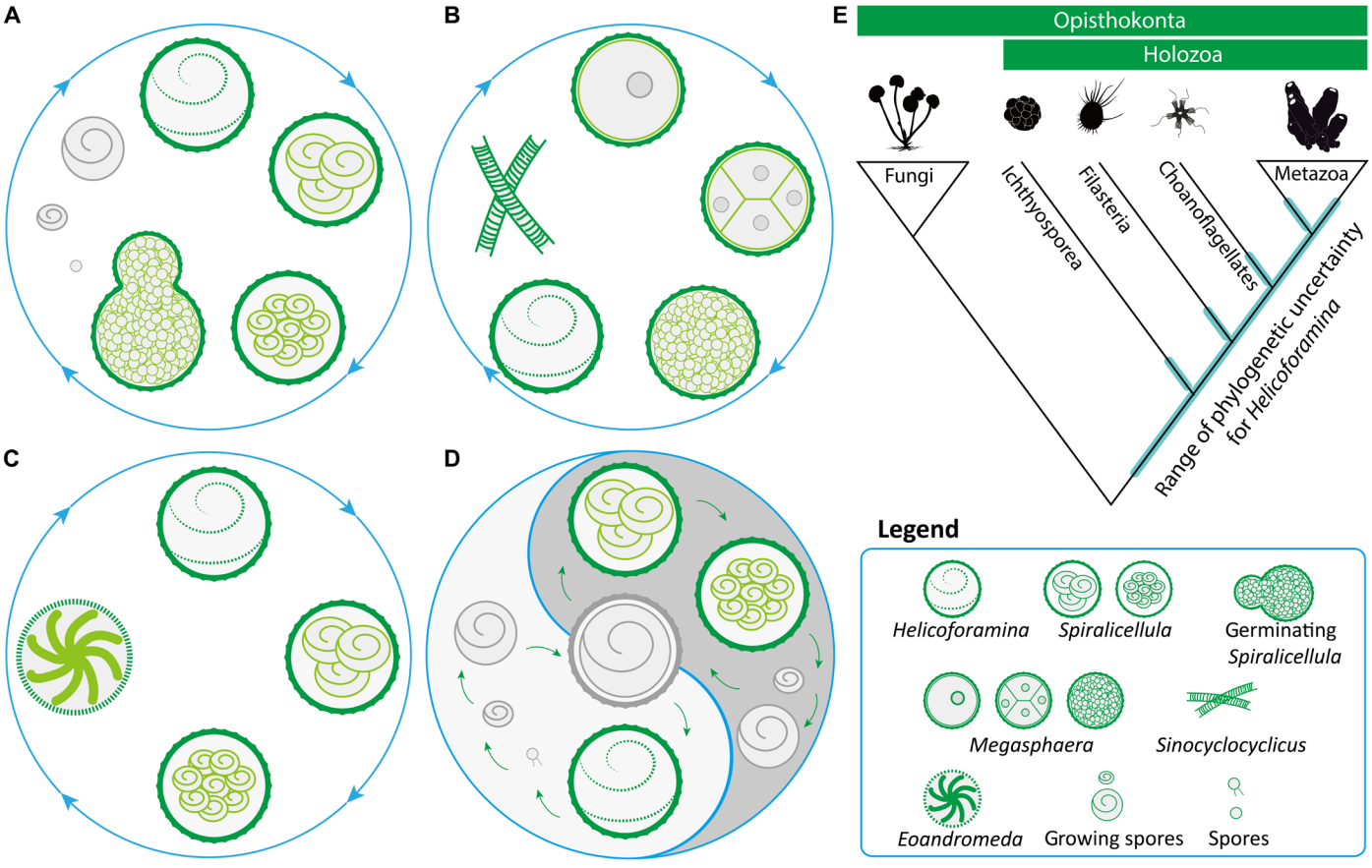

Fig. 2. Proposed life cycles and phylogenetic positions for *Helicoforamina*. (A to D) Various life cycles for *Helicoforamina* proposed previously. (**A**) *Helicoformina* as one-cell egg of multicellular *Spiralicellula* (*4*). (**B**) *Helicoforamina* as an embryo of tubular microfossils *Sinocyclocyclicus* at postblastula stage (*8*). (**C**) *Helicoforamina* as an embryo of *Eoandromeda (16)*. (**D**) *Helicoforamina* and *Spiralicellula* as stages in alternating sexual (yin) and asexual (yang) phases of the life cycle of a chlorophyceaean alga (*7*). (**E**) A simplified phylogenetic tree of Holozoa, with fungi as the outgroup. The potential placements for *Helicoforamina* in the holozoan tree are indicated in cyan.

blastomeres into a *Helicoforamina* helical inner body (*8*). Tang *et al.* (*16*) suggested that *Helicoforamina* and *Spiralicellula* represent embryos of *Eoandromeda*, which they compared to adult octocorals and ctenophores (Fig. 2C). Wang *et al.* (*17*) rejected linking *Helicoforamina* and *Sinocyclocyclicus* on the basis of the autapomorphic helical structure, preferring to interpret *Helicoforamina* as a foraminifer, with the helically arranged pores representing sites for extrusion of pseudopodia. Zhang and Pratt (*7*) interpreted *Helicoforamina* and *Spiralicellula* as stages in alternating sexual and asexual life cycles of a chlorophyceaean alga (Fig. 2D), based principally on the inferred ecology of the environment in which they lived, their comparable abundance, and the resemblance of their thick ornamented cyst wall to the zygospores of Chlorophyceae.

In large part, this phylogenetic controversy arises because so little is known about the biology of *Helicoforamina*. Tomographic analyses of *Megasphaera* and of *Spiralicellula* have yielded further insights into their developmental biology, demonstrating unequivocally that, like *Megasphaera*, cells in *Spiralicellula* were nucleated and underwent binary and equal reductive palintomy (*3*, *4*). However, there have been no further insights into the biology of *Helicoforamina* and, thus, no data to marshal in tests of a developmental link to co-occurring taxa. To remedy this deficit, we undertook tomographic analysis of a collection of 327 specimens *of Helicoforamina*, revealing specimens that harbor cells (Figs. 3 and 4) arranged either into a tight tetrad (Fig. 3, D to H), an octad (Fig. 3, I to K), or hundreds of rounded and dispersed cells (Fig. 4, A to D). These are equivalent to the early palintomic stages of *Megasphaera* and *Spiralicellula*; hence, we reject the hypothesis of a developmental link between *Helicoforamina*, *Megasphaera,* and *Spiralicellula*, which must, rather, represent equivalent developmental stages of disparate taxa. Furthermore, our results provide conclusive evidence that the similar nature of the envelope ornament, which inspired synonymy of *Megasphaera* and *Helicoforamina*, belies a diversity of taxa. Thus, the diversity of taxa represented by the Weng'an assemblage must be much greater than previously thought.

RESULTS

We obtained submicrometer-scale tomographic data for more than 300 specimens of *Helicoforamina wenganica* representative of known morphological and taphonomic range, based on a rich fossil assemblage from "54 Quarry" in the Baiyan-Gaoping anticline of Weng'an County, Guizhou Province, South China (*18*). Specimens vary in terms of the extent of the helically arranged pits, canal, or groove, but also in terms of the preserved thickness of the outer wall (Figs. 1 and 3 to 6) and the degree of postmortem shrinkage (e.g.,

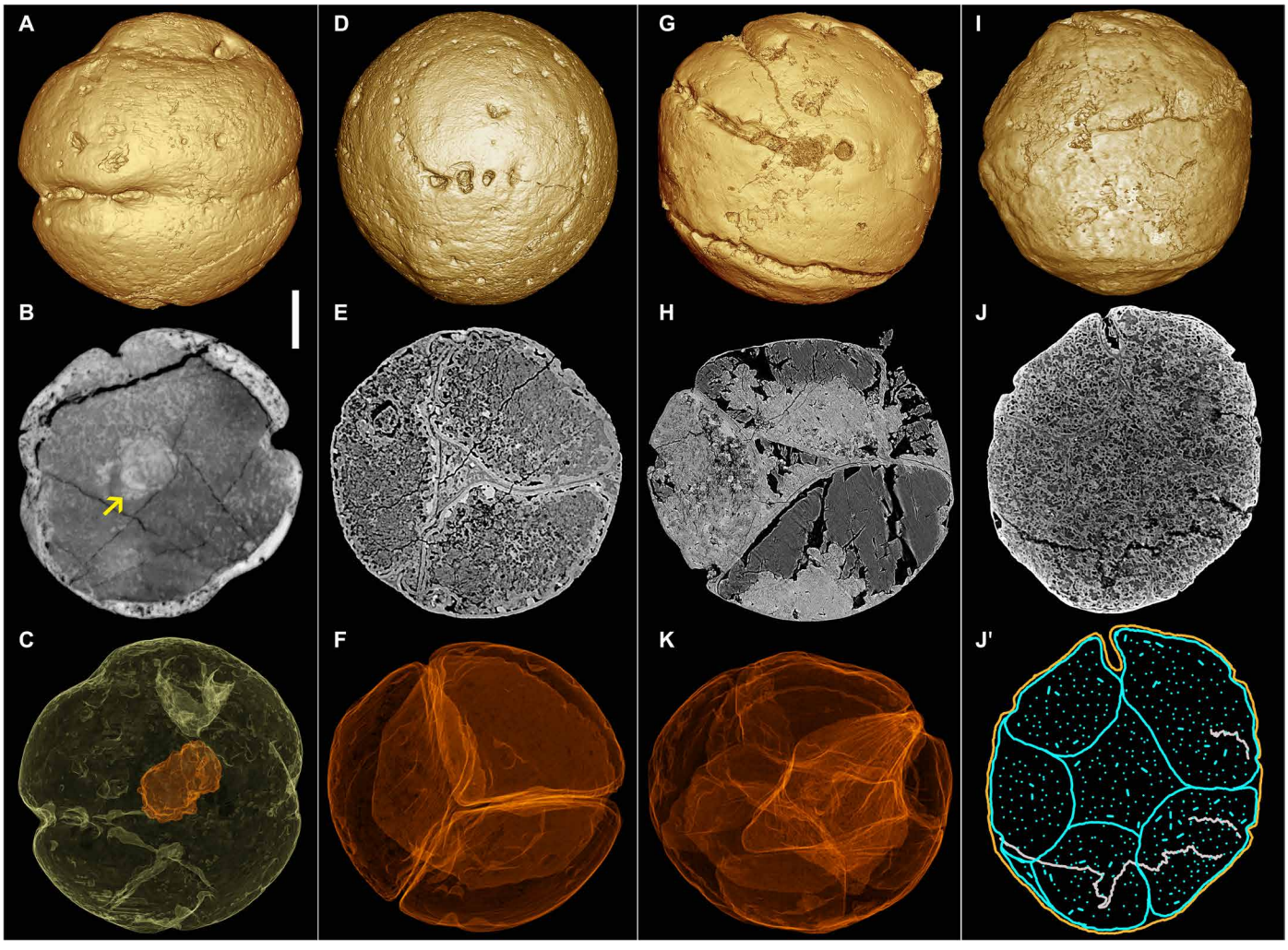

Fig. 3. *Helicoforamina* at early developmental stages. (**A** to **C**) NIGP173064, single-cell stage. (**D** to **F**) NIGP173065, four-cell stage. (**G** and **H**) NIGP173066, four-cell stage. (**I** to **K**) NIGP173067, eight-cell stage. (A, D, G, and I) Surface renderings. (B, E, H, and J) Virtual sections showing internal structures. (C, F, and K) Transparent models showing nucleus and cells. (J') A sketch of (J), showing the cell boundaries. The arrow in (B) indicates the nucleus. Scale bars, (A to C) 174 μm, (D to F) 120 μm, and (G to K) 145 μm.

Fig. 5A). In the best-preserved specimens, the outer wall is thick (12 to 31 μm) and multilayered (e.g., Fig. 1, I to L and N to Q), but in others, the outer wall is incomplete (e.g., Fig. 1M) or delaminated with intervening voids (e.g., Fig. 1N, Q, and S) or void-filling diagenetic cements (e.g., Fig. 5, B and J). Consequently, the characteristic helically arranged channel, canal, or pores of *Helicoforamina* vary in the extent to which they penetrate the outer wall, incompletely in well-preserved specimens and completely in specimens where the inner layers are absent. In the best-preserved specimens, the inner surface of the outer wall is unaffected by the helical channel, canal, or pores (Fig. 1, N, O, and S), or the inner surface exhibits a broad convexity to accommodate an associated increase in the thickness of the outer wall (e.g., Fig. 1, P and T). Where the outer wall has delaminated (e.g., Fig. 1, N and S), it can exhibit much greater variation in thickness, and this has a concomitant impact on the morphology of natural endocasts, which vary from spherical to a more approximately helical (Fig. 6). The helical endocasts are an artifact of differential compaction of a delaminated outer wall; the outer wall retains its thickness around the helical canals but is otherwise compacted, resulting in convex bulges into the central lumen associated with the helical canal (Fig. 6, I to L). In many specimens, the outer wall is entirely absent, or there is a pseudowall composed of a late diagenetic crust in a more highly x-ray attenuating mineral phase (e.g., Fig. 5, C and K). The helical channel or canal can be preserved; nevertheless (Fig. 5, C to G and K to O), given that no aspects of internal biology are preserved in these specimens, we presume that the histology of the outer wall is absent because it is not preserved rather than because it has not developed.

Beneath the outer wall, the specimens are invariably solid and almost always show evidence of multiple phases of void-filling cement, manifest as mineral phases with different x-ray attenuation profiles. These vary from fine-grained and largely homogenous (Fig. 5, E and M) to clotted fabrics (Fig. 6, E to H), to layered anatomosing geode-like void-filling patterns of calcium phosphate mineralization (Fig. 5, F and N). Some specimens retain open voids (e.g., Fig. 5, G and O), while in others, such spaces are filled with macroscopic crystals of calcite or dolomite (e.g., Fig. 5, B and J); intermediates (e.g., Fig. 5, C, K, H, and P) demonstrate that this difference reflects the degree of dissolution of the carbonate matrix during the acetic acid recovery of the specimens. A small number of

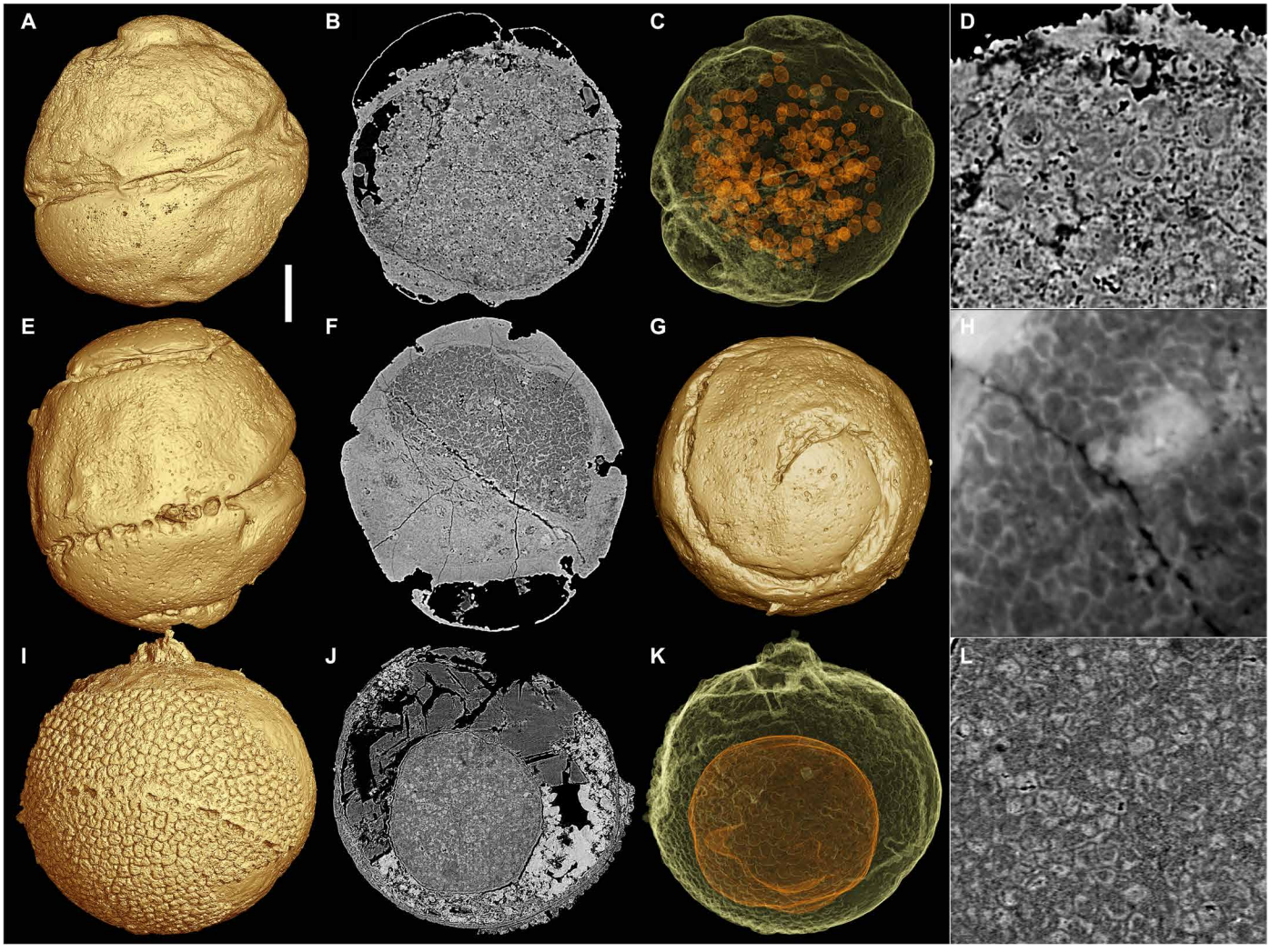

Fig. 4. *Helicoforamina* at later developmental stages. (**A** to **C**) NIGP173068; (**E** to **G**) NIGP173069; (**I** to **K**) NIGP173070. (A, E, G, and I) Surface renderings. (B, F, and J) Virtual sections. (C and K) Transparent models showing internal cells or shrunk inner bodies. (**D**, **H**, and **L**) Close-up views of (B), (F), and (J), respectively, showing multicellular structures. Scale bars, (A and C) 150 μm, (B) 142 μm, (D) 50 μm, (E and G) 140 μm, (F) 170 μm, (H) 42 μm, (I to K) 165 μm, and (L) 45 μm.

specimens also include large pyrite crystals within the natural endocast, distinguished by crystal habit and high x-ray attenuation.

Some specimens show evidence of inner bodies smaller than the inner volume of the outer wall, but which trace its shape, reflecting postmortem shrinkage [e.g., Figs. 1 (K, L, P to R) and 4 (I to K)]; the intervening volume is occupied by coarse void-filling cement, while the inner body is more finely crystalline, characteristic of mineralization of an original biological substrate (Fig. 1, P, Q, and U) (*19*). In some specimens, centrifugal lining of the void beneath the inner surface of the outer wall can create the impression of a thickened outer wall, but this is a diagenetic void-filling mineral artifact (e.g., Fig. 1, N and S). Sometimes, the shrunken inner body is surrounded by a delaminated and incomplete outer wall, the matrix between which has subsequently been void filled (Figs. 1, L and Q, and 4, I to K).

Sixteen specimens preserve biological structures inside the outer envelope (Figs. 3, 4, and 6). These include two specimens in which a membrane-bound, large intracellular structure is centrally located (Fig. 3B) and shows similar preservation and size akin to the nuclei of *Megasphaera* and *Spiralicellula*, indicating that they are preserved at a single-cell stage of development (Fig. 3, A to C). Four specimens preserve the walls of four large cells, arranged tetrahedrally (Fig. 3, D to H), and two additional specimens preserve eight large cells in a coordinated arrangement (Fig. 3, I to K). These large cells are of equal size within each specimen and fill more or less fully the space enclosed by the outer wall. A couple of specimens preserve small spheroids in a manner akin to the cells in specimens of "*Megaclonophycus*-stage" *Megasphaera* (e.g., Fig. 4, A to D), where the cell membrane exhibits evidence of centripetal and/or centrifugal mineralization (*19*). The spheroidal morphology of the cells and their discrete distribution suggest that if they were once associated, they have been disaggregated. Last, four specimens preserve polygonal cell–like structures, circa 10 to 20 μm in diameter, around the periphery of the inner body (e.g., Fig. 4, E to H) or completely fill the shrunken inner body (e.g., Fig. 4, I to L). Normally, only the cell membranes are preserved and the cells themselves are empty or filled by homogeneous mineralization.

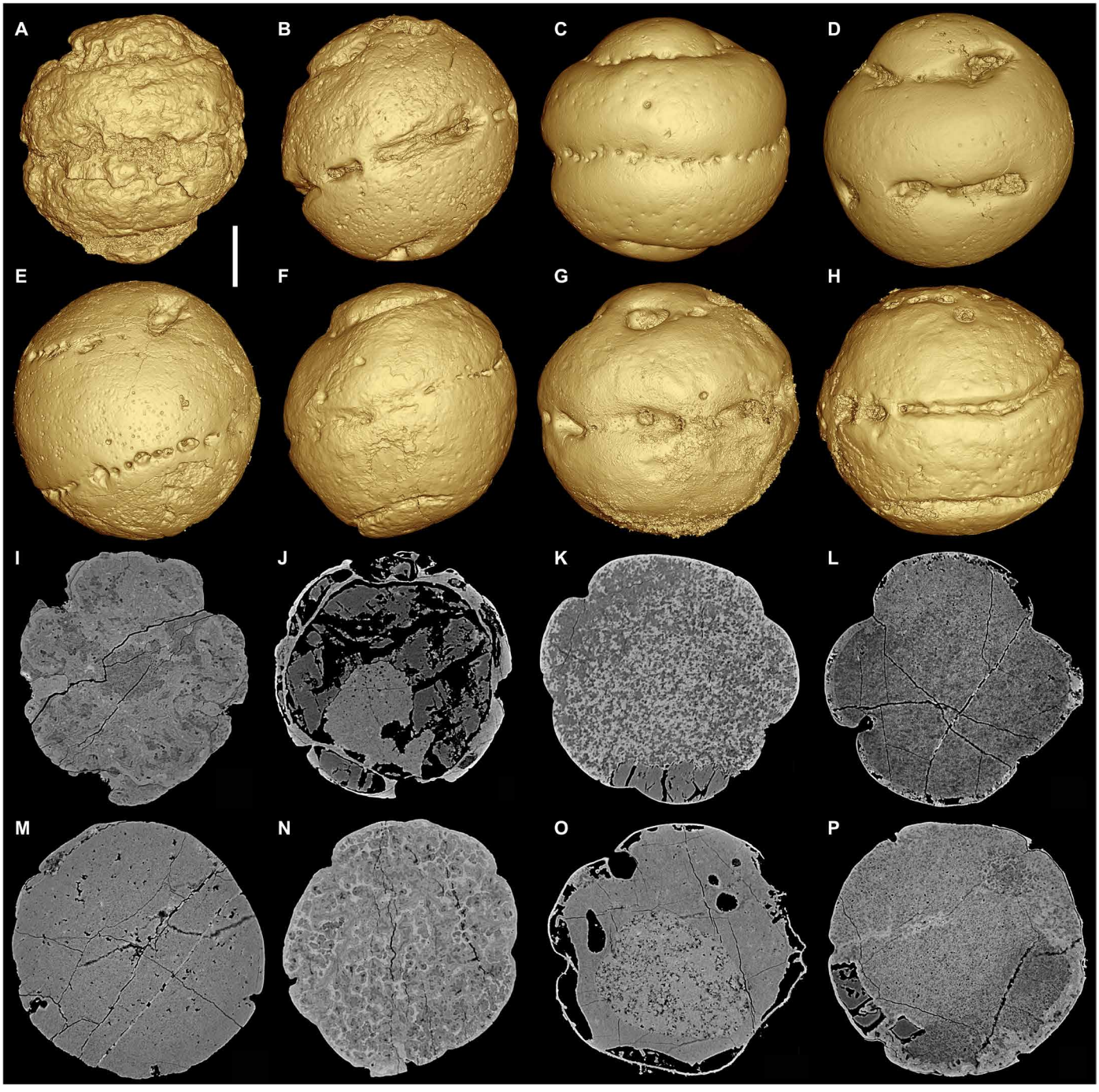

Fig. 5. Taphonomy of *Helicoforamina*. (**A**) NIGP173071. (**B**) NIGP173072. (**C**) NIGP173073. (**D**) NIGP173074. (**E**) NIGP173075. (**F**) NIGP173076. (**G**) NIGP173077. (**H**) NIGP173078. (A to H) Surface renderings. (**I** to **P**) Virtual sections of (A) to (H), respectively, showing internal structures. Scale bars, (A, B, I, and J) 200 μm, (C and K) 175 μm, (D and L) 187 μm, (E and M) 170 μm, (F and N) 185 μm, and (G, O, H, and P) 165 μm.

DISCUSSION

The relationship between *Helicoforamina* and other components of the Weng'an biota

Our data allow us to constrain existing interpretations of the biology of *Helicoforamina* and assess the hypotheses on its relationship to co-occurring *Megasphaera, Sinocyclocyclicus,* and *Spiralicellula*. The available evidence indicates that the known forms of *Helicoforamina* do not represent late developmental stages. The presence of one-, four-, and eight-celled developmental stages reflects an early stage of development, compatible with successive rounds of binary reductive palintomy from a single mother cell. Additional specimens that preserve evidence of hundreds to thousands of cells indicate successive rounds of cell division and, therefore, a protracted period of development within the helical envelope; by comparison, metazoan

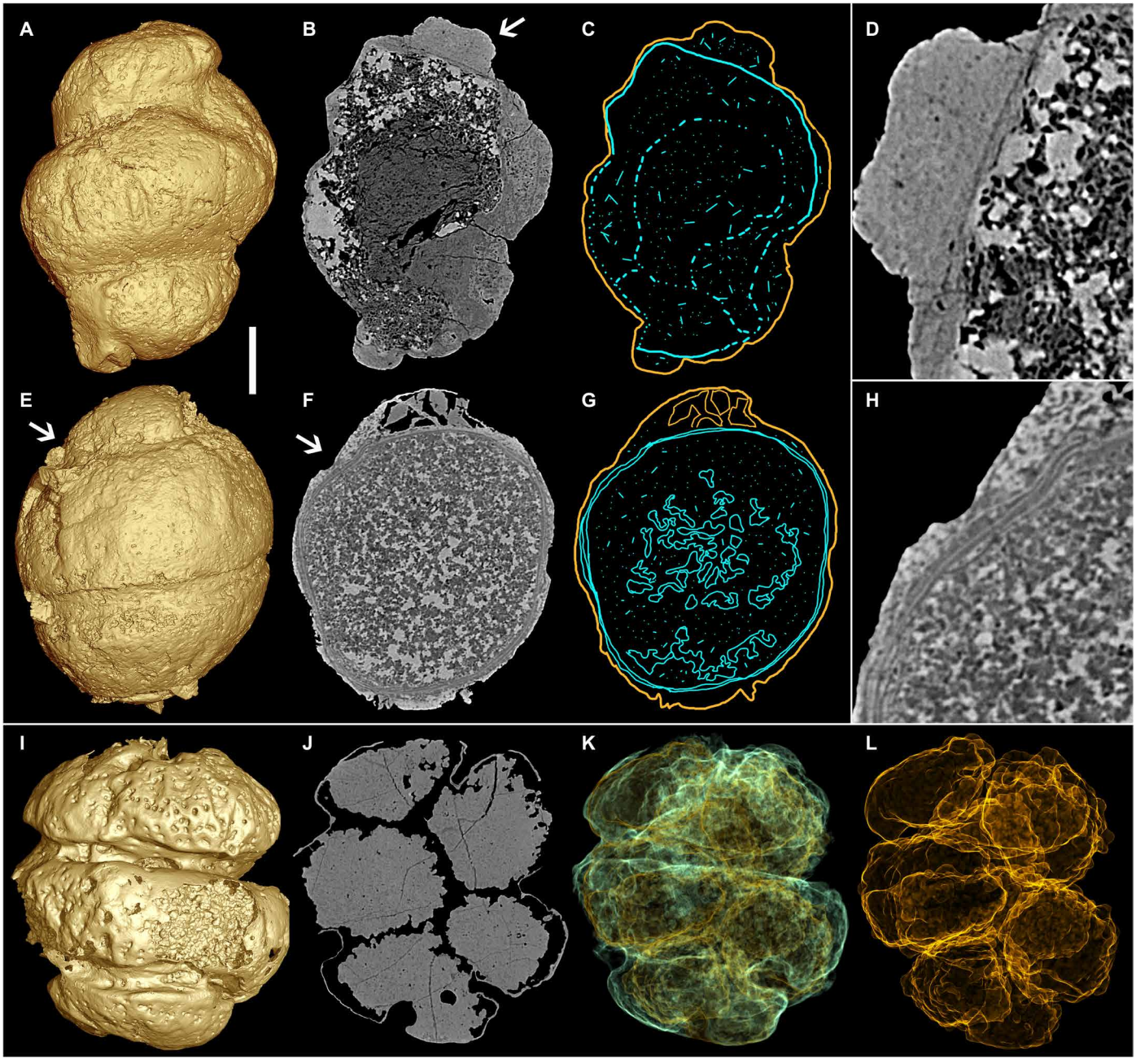

Fig. 6. Pseudo-uncoiling *Helicoforamina*. (**A**) NIGP173079. (**E**) NIGP173080. (**I**) NIGP173081. (A, E, and I) Surface renderings. (**B**, **F**, and **J**) Virtual sections of (A), (E), and (I), respectively. (**C** and **G**) Sketches of (B) and (F), respectively, showing the relationship between the inner wall of the envelopes and the inner bodies. The arrows indicate the positions of the groove. (**D** and **H**) Close-up views of (B) and (F), respectively, showing the boundaries between the inner wall and inner bodies. (**K**) Transparent model of (I), showing internal cells. (**L**) Transparent model of internal cells. Scale bars, 50 μm for (D) and (H), 150 μm for the others.

embryos have ordinarily undergone differentiation and epithelialization at comparable cell stages (*20*). The partially uncoiled morphology of the early cleaving specimens (e.g., Fig. 6, I to L) suggests that the putative prehatchling is a taphonomic artifact, resulting from the distortion of the inner surface of the outer wall, which gives rise to natural endocasts with broad and deeply excavated helical grooves that reflect the position of the relatively uncompacted helical canal. The differential preservation of the helical groove, canal, and pores indicates that, for the known developmental stages, these structures were limited to the wall of the envelope. Hence, they could not have served a role in gas exchange between the interior and exterior (*8*), nor could they represent sites of pseudopodial extension (*17*).

It is tempting to interpret the different states of the helical structure, viz as a groove, canal, and series of pores, as a pattern of development. There are specimens in our collection in which a helical groove is only very weakly developed (e.g., Fig. 1J). However, there is insufficient

independent evidence of developmental polarity from the cells preserved inside to justify such an interpretation.

Despite their similarity, we can reject the hypothesis of a developmental link between *Helicoforamina* and *Megasphaera* (*4*, *8*, *12*). This is because the tetrahedral and octahedral arrangement of cells in *Helicoforamina* (Fig. 3) and the "*Parapandorina* stage" of *Megasphaera* (*9*, *20*) demonstrates that they represent equivalent developmental stages and, hence, the morphological distinctiveness of their envelope morphology precludes the possibility that they are derived from the same organism.

Similarly, we reject the hypothesis of homology between *Helicoforamina* and *Spiralicellula* (*4*, *7*, *8*, *16*) because the material basis for this hypothesis, that the spiral internal bodies of *Helicoforamina* resemble the component cells of *Spiralicellula*, is a taphonomic artifact of preservation in *Helicoforamina*. Hence, anticipated intermediate stages (*8*, *12*) between *Helicoforamina* and *Spiralicellula* have not been recovered despite extensive sampling by us and others. No helical structures develop on the surface of the large dividing cells of *Helicoforamina,* which is distinct from the morphology of the dividing cells of *Spiralicellula*, neither is there evidence of helical canals or a sequence of pores on the envelopes of *Spiralicellula*. Last, the (taphonomically derived) inner bodies of *Helicoforamina* differ in scale from the co-occurring microtubular fossils, such as *Sinocyclocyclicus* (*21*). The resemblance of *Helicoforamina* to these fossils is superficial and cannot be interpreted as indicative of affinity.

The holozoan affinity of *Helicoforamina*

Previous attempts to resolve the affinity of *Helicoforamina* have relied upon a developmental association of *Helicoforamina* with other embryo-like taxa in the Weng'an biota. With these links rejected, we must also reject the associated interpretations of affinity. Instead, we attempt to resolve the affinity of *Helicoformina* based only on its preserved anatomy and development. The characteristics of binary reductive palintomy of cells with flexible walls and Y-shaped cell interfaces, enclosed within a complex multilaminate cyst wall, allow us to conclude minimally that these specimens of *Helicoforamina* reflect coordinately dividing multicelled stages in a broader life cycle. The similarity between *Helicoforamina* and *Megasphaera* in the ornament and complex histological structure of the outer wall of, as well as the well-preserved nuclei in some specimens, also allows us to conclude that *Helicoforamina* is a eukaryote, at the very least.

In the history of interpretations of the Weng'an biota, Y-shaped cell interfaces are seen also in *Megasphaera*, where they have been commonly interpreted to indicate animal affinity (*5*, *12*, *22*); however, Y-shaped cell interfaces are encountered in embryo-like conformations of cells in diverse eukaryotes including ciliates, rhodophytes, and nonmetazoan holozoans (*18*). Yin *et al.* (*13*) reviewed the diversity of embryo-like developmental stages that occur in eukaryotes. Among these, the known developmental stages of *Helicoforamina* bear a strong resemblance to the early binary reductive palintomic stages of rhodophyte embryos (*23*, *24*). However, the resemblance is limited to the early stages of palintomy in *Helicoforamina*, since rhodophytes undergo morphogenesis after just four or five rounds of palintomy (*23*–*25*), which is inconsistent with the fact that *Helicoforamina* stages can have hundreds of cells. Furthermore, while *Helicoforamina* begins palintomy within its multilaminate ornate cyst, rhodophyte embryos are initially naked, only later developing an irregular mucilaginous sheath (*26*). Given such simple clusters of cells, it is conceivable that the grade of organization exhibited by *Helicoforamina* could have evolved as a multicellular stage in any, or even many, lineages of eukaryote. However, all of the eukaryote lineages that have evolved embryo-like stages in their life cycle are generally more similar to each other than any one of them is to *Helicoforamina*, with the exception of holozoans [see (*13*) for *Caveasphaera*]. It is the combination of recurrent rounds of coordinated cell division exhibited by (and inferred in) *Helicoforamina*, developing within a relatively complex multilaminate cyst, that sets it apart, since all other nonholozoan multicellular eukaryote life history stages undergo rapid morphogenesis after just one or a handful of rounds of reductive division (*13*). Certainly, nonmetazoan holozoans such as ichthyosporeans and filastereans generate multicelled stages within their respective life cycles (*27*–*29*), some with a degree of coordination that goes beyond that currently known in *Helicoforamina* (*30*). However, the structure of the enveloping cyst in *Helicoforamina* is itself more complex than is seen in nonmetazoan holozoans.

This same debate has played out over phylogenetic interpretations of *Megasphaera* and *Spiralicellula*. Like *Helicoforamina*, they exhibit patterns of development compatible with early cleavage stages of animal embryos, but these may be shared primitive characteristics of holozoan life cycles (*4*). Chen *et al.* (*5*) attempted to identify definitive metazoan characteristics, including cell differentiation, germ-soma separation, and apoptosis. Evidence of cell differentiation manifests as diad cells among monads, but this is more likely a consequence of asynchronous cell division (*20*), and elongate peripheral cells, which can also be interpreted as a consequence of postmortem loss of cell adhesion, inflation, and the constraints of an enclosing envelope (*31*). Germ-soma separation is evidenced by local clusters of distinctly smaller cells that are envisaged as product of the diad cells, but there is no evidence of this developmental relationship, and identical cell clusters occur in co-occurring multicellular algae, suggesting an exogenous origin (*32*). Conversely, Huldtgren *et al.* (*4*) attempted to reject a metazoan affinity in demonstrating that the early palintomically dividing cells of *Megasphaera* and *Spiralicellula* result ultimately in a peanut-shaped multicellular body composed of hundreds of thousands of cells that are shed to the environment. However, although a convincing case can be made for a developmental link between the *Parapandorina* stage (with tens of cells) and the *Megaclonophycus* stage (composed of hundreds to thousands of cells), the search for intermediates that might bridge the developmental gap to the peanut-shaped stages, or peanut-shaped stages retaining the *Megasphaera*-grade envelope, has not been fruitful (*12*, *33*). Hence, it is difficult to rationalize whether *Megasphaera* and *Spiralicellula* preserve only holozoan symplesiomorphies because developmental stages exhibiting metazoan synapomorphies have not been preserved [a stemward slippage (*34*) filter of developmental stages] or whether it is because they represent nonmetazoan holozoans. The same holds true for *Helicoforamina*, which, like *Megasphaera* and *Spiralicellula*, might most safely be interpreted as total-group holozoans, i.e., on the available evidence, it is not possible to discriminate definitively between a nonmetazoan holozoan and metazoan interpretation (Fig. 2E). A similar conclusion was reached for co-occurring *Caveasphaera*, which is known from a much more extensive series of developmental stages and which exhibits a more complex pattern of embryology (*13*).

Cryptic diversity in the Weng'an biota and an influence of heterogeneous environmental conditions on the evolution of development

The similarity in the envelope ornament and histology of *Helicoforamina* and *Megasphaera*, as well as *Spiralicellula* and *Caveasphaera*, provides

conclusive evidence that this character is not in and of itself informative, either of affinity to living clades or as a basis for grouping the disparate developmental stages preserved in the Weng'an biota. This is important because this character has been used to rationalize most of such fossils as representing developmental stages of a single organism (e.g., *4*, *7*, *8*, *12*), diminishing perception of the diversity of organisms preserved in this unique window on early Ediacaran marine life. It also exposes to scrutiny why such a diversity of developmental stages of disparate organisms are preserved at all and belies the view that developmental stages of a single organism could be so abundantly fossilized (*7*, *35*). The convergent evolution of an encysted developmental stage probably explains the preservation of this same developmental stage across diverse taxa because experiments have shown that encysted embryos have elevated fossilization potential compared with other developmental stages (*36*). Further sampling is required to establish the extent of the diversity and developmental biology of Ediacaran marine life in the Weng'an biota that has been obscured hitherto by a common envelope morphology and structure.

In the interim, it is pertinent to consider why such diverse organisms should have converged on such similar cyst walls of comparable size, multilaminate structure, and surface ornamentation. The comparatively large size of these and other early developmental stages [e.g., *Sporosphaera* (*37*)] implies maternal investment of energy stores to facilitate long gestation and direct development, and preserved intracellular lipid vesicles have been described from *Spiralicellula* and *Megasphaera* (*20*). Comparable cyst walls have been interpreted as diapause stages in the embryology of early metazoans (*38*, *39*). Regardless of their affinity, these factors suggest an adaptation to the spatially and temporally heterogeneous conditions that occurred in shallow marine environments through much of the Ediacaran (*40*). Although the Weng'an biota is interpreted to have been deposited under oxygenated conditions, conditions would have been especially challenging for benthic organisms or life stages given the strong and fluctuating redox conditions associated with the attendant sedimentary phosphogenesis (*12*).

Our analysis of the developmental biology of *Helicoforamina* also highlights the challenge of reconstructing the embryology and life cycle of fossil organisms, distinguishing whether disparate specimens represent different developmental stages of a single organism, or comparable versus different developmental stages of different organisms. In this instance, it has been possible to rationalize these competing interpretations because the Ediacaran Weng'an biota is so abundantly preserved. Fossilized embryonic stages are much rarer in the other deposits in which they are known (*41*), rendering the developmental relationships among specimens less open to testing and, therefore, less secure, limiting our ability to test hypotheses of developmental evolution otherwise based solely on phylogenetic inference of the life histories of living organisms.

CONCLUSIONS

We studied a rich collection of specimens of *Helicoforamina wenganica* from the early Ediacaran Weng'an biota to test established hypotheses on the biological affinity and developmental relationship of this taxon to other, better known taxa from the deposit. We describe its taphonomy and demonstrate that putative prehatchling stages are taphonomic artifacts. Further, rare specimens of *Helicoforamina* preserve cells inside, indicative of coordinated and equal palintomy. These data allow us to reject all established hypotheses that propose a developmental relationship of this taxon to other taxa (Fig. 2, A to D); *Helicoforamina* is a distinct taxon, not merely a distinct developmental stage. This evidences a much richer diversity of taxa and developmental stages preserved in this unique window on early Ediacaran marine life than has been perceived hitherto. We constrain the affinity of *Helicoforamina* to Holozoa; we cannot discriminate between nonmetazoan and metazoan holozoan affinities (Fig. 2E). The diverse Weng'an biota shares similarly ornamented encysted developmental stages as an adaptation to the temporally and spatially heterogeneous nature of Ediacaran shallow marine environments.

MATERIALS AND METHODS

We obtained an abundant collection of *Helicoforamina wenganica* through acetic acid dissolution of phosphoritic dolomite from the Upper Grey Facies (Units 4b; *18*) of the Doushantuo Formation at 54 Quarry, in the Baiyan-Gaoping anticline of Weng'an County, Guizhou Province, Southwest China. For further information on the geographic location, stratigraphy, and environmental interpretation, see Cunningham *et al.* (*18*) and references therein. The Weng'an assemblage is dominated by embryo-like fossils with a cerebral, fractal, or dimpled surface ornamentation that have been variably attributed to *Megasphaera*, *Tianzhushania*, and *Yintianzhushania*. Given the implications of our study that there is a cryptic diversity of taxa that cannot be discriminated on the basis of their surface ornamentation, in the text, we refer to them all to *Megasphaera*, pending establishment of criteria on which they may be consistently discriminated.

The best preserved of these were subjected to tomographic analysis using a Carl Zeiss Xradia 520 Versa x-ray tomographic microscope at Nanjing Institute of Geology and Palaeontology, Chinese Academy of Sciences (NIGPAS), and synchrotron radiation x-ray tomographic microscopy (srXTM) at the X02DA TOMCAT beamline of the Swiss Light Source (SLS; Paul Scherrer Institute, Villigen, Switzerland) and BM5 beamline of the European Synchrotron Radiation Facility (ESRF; Grenoble, France). Measurements on the Xradia instrument were obtained with an operating voltage of 50 kV, LE1 filter, and 4× objective yielding isotropic voxel dimensions of 0.82 to 1.1 μm, collecting 3001 projections through a rotation of 360°. srXTM data were obtained using 10× and 20× objective lenses at SLS (yielding reconstructed tomographic data with voxel dimensions of 0.65 and 0.325 μm, respectively) or 10× objective lens at ESRF (voxel dimension of 0.75 μm) at energy levels of 15 to 20 keV and exposure times of 50 to 400 ms. Projections (1501) were taken equianglularly through 180° of rotation within the beam. Projections were postprocessed and rearranged into flat- and dark-field–corrected sinograms, and reconstruction was performed on a 60-core Linux PC farm, using a highly optimized routine based on the Fourier transform method and a regridding procedure (*42*). Slice data were analyzed and manipulated using VGStudioMax (www.volumegraphics.com). Given that the x-rays from the synchrotron sources are monochromatic, differences in contrast in the resulting tomographic slices reflect the densities of the fossil materials they pass through.

View/request a protocol for this paper from *Bio-protocol*.

REFERENCES AND NOTES

1. M. dos Reis, Y. Thawornwattana, K. Angelis, M. J. Telford, P. C. Donoghue, Z. Yang, Uncertainty in the timing of origin of animals and the limits of precision in molecular timescales. *Curr. Biol.* **25**, 2939–2950 (2015).

2. D. H. Erwin, M. Laflamme, S. M. Tweedt, E. A. Sperling, D. Pisani, K. J. Peterson, The Cambrian conundrum: Early divergence and later ecological success in the early history of animals. *Science* **334**, 1091–1097 (2011).
3. Z. Yin, J. A. Cunningham, K. Vargas, S. Bengtson, M. Zhu, P. C. J. Donoghue, Nuclei and nucleoli in embryo-like fossils from the Ediacaran Weng'an Biota. *Precambrian Res.* **301**, 145–151 (2017).
4. T. Huldtgren, J. A. Cunningham, C. Yin, M. Stampanoni, F. Marone, P. C. J. Donoghue, S. Bengtson, Fossilized nuclei and germination structures identify Ediacaran "animal embryos" as encysting protists. *Science* **334**, 1696–1699 (2011).
5. L. Chen, S. Xiao, K. Pang, C. Zhou, X. Yuan, Cell differentiation and germ–soma separation in Ediacaran animal embryo-like fossils. *Nature* **516**, 238–241 (2014).
6. Z. Yin, M. Zhu, D. J. Bottjer, F. Zhao, P. Tafforeau, Meroblastic cleavage identifies some Ediacaran Doushantuo (China) embryo-like fossils as metazoans. *Geology* **44**, 735–738 (2016).
7. X.-G. Zhang, B. R. Pratt, Possible algal origin and life cycle of Ediacaran Doushantuo microfossils with dextral spiral structure. *J. Paleo.* **88**, 92–98 (2014).
8. S. Xiao, J. W. Hagadorn, C. Zhou, X. Yuan, Rare helical spheroidal fossils from the Doushantuo Lagerstätte: Ediacaran animal embryos come of age? *Geology* **35**, 115–118 (2007).
9. S. Xiao, Y. Zhang, A. H. Knoll, Three-dimensional preservation of algae and animal embryos in a Neoproterozoic phosphorite. *Nature* **391**, 553–558 (1998).
10. S. Xiao, A. H. Knoll, Phosphatized animal embryos from the Neoproterozoic Doushantuo Formation at Weng'an, Guizhou, South China. *J. Paleo.* **74**, 767–788 (2000).
11. S. Xiao, C. Zhou, P. Liu, D. Wang, X. Yuan, Phosphatized acanthomorphic acritarchs and related microfossils from the Ediacaran Doushantuo Formation at Weng'an (South China) and their implications for biostratigraphic correlation. *J. Paleo.* **88**, 1–67 (2014).
12. S. Xiao, A. D. Muscente, L. Chen, C. Zhou, J. D. Schiffbauer, A. D. Wood, N. F. Polys, X. Yuan, The Weng'an biota and the Ediacaran radiation of multicellular eukaryotes. *Natl. Sci. Rev.* **1**, 498–520 (2014).
13. Z. Yin, K. Vargas, J. Cunningham, S. Bengtson, M. Zhu, F. Marone, P. Donoghue, The early Ediacaran *Caveasphaera* foreshadows the evolutionary origin of animal-like embryology. *Curr. Biol.* **29**, 4307–4314.e2 (2019).
14. S. Xiao, X. Yuan, A. H. Knoll, Eumetazoan fossils in terminal Proterozoic phosphorites? *Proc. Natl. Acad. Sci. U.S.A.* **97**, 13684–13689 (2000).
15. J. Y. Chen, P. Oliveri, F. Gao, S. Q. Dornbos, C. W. Li, D. J. Bottjer, E. H. Davidson, Precambrian animal life: Probable developmental and adult cnidarian forms from Southwest China. *Dev. Biol.* **248**, 182–196 (2002).
16. F. Tang, C. Yin, B. Stefan, P. Liu, Z. Wang, L. Gao, Octoradiate spiral organisms in the Ediacaran of South China. *Acta Geol. Sin.* **82**, 27–34 (2008).
17. D. Wang, L. Chen, Q. Tang, K. Pang, Spheroidal fossils with helically distributed spores from the Ediacaran Doushantuo phosphorites of Weng'an, Guizhou. *Acta Palaeontologica Sinica* **51**, 88–95 (2012).
18. J. A. Cunningham, K. Vargas, Z. Yin, S. Bengtson, P. C. J. Donoghue, The Weng'an Biota (Doushantuo Formation): An Ediacaran window on soft-bodied and multicellular microorganisms. *J. Geol. Soc. London* **174**, 793–802 (2017).
19. J. A. Cunningham, C.-W. Thomas, S. Bengtson, S. L. Kearns, S. Xiao, F. Marone, M. Stampanoni, P. C. J. Donoghue, Distinguishing geology from biology in the Ediacaran Doushantuo biota relaxes constraints on the timing of the origin of bilaterians. *Proc. Biol. Sci.* **279**, 2369–2376 (2012).
20. J. W. Hagadorn, S. Xiao, P. C. J. Donoghue, S. Bengtson, N. J. Gostling, M. Pawlowska, E. C. Raff, R. A. Raff, F. R. Turner, Y. Chongyu, C. Zhou, X. Yuan, M. B. McFeely, M. Stampanoni, K. H. Nealson, Cellular and subcellular structure of Neoproterozoic animal embryos. *Science* **314**, 291–294 (2006).
21. W.-C. Sun, Z.-J. Yin, P. Donoghue, P.-J. Liu, X.-D. Shang, M.-Y. Zhu, Tubular microfossils from the Ediacaran Weng'an Biota (Doushantuo Formation, South China) are not early animals. *Palaeoworld* **28**, 469–477 (2019).
22. S. Xiao, Mitotic topologies and mechanics of Neoproterozoic algae and animal embryos. *Paleobiology* **28**, 244–250 (2002).
23. G. Wang, C. Jiang, S. Wang, X. Wei, F. Zhao, Early development of *Grateloupia turuturu* (Halymeniaceae, Rhodophyta). *Chinese J. Oceanol. Limnol.* **30**, 264–268 (2012).
24. K. M. Michetti, L. A. Martín, P. I. Leonardi, Carpospore release and sporeling development in Gracilaria gracilis (Gracilariales, Rhodophyta) from the southwestern Atlantic coast (Chubut, Argentina). *J. Appl.Phycol.* **25**, 1917–1924 (2013).
25. V. Krishnamurthy, in *Reproductive Biology of Plants*, B. M. Johri, P. S. Srivastava, Eds. (Springer, Heidelberg, Berlin, 2001), pp. 57–95.
26. I. Tsekos, The ultrastructure of carposporogenesis in *Gigartina teedii* (Roth) Lamour. (*Gigartinales, Rhodophyceae*): Gonimoblast cells and carpospores. *Flora* **174**, 191–211 (1983).
27. M. Ferrer-Bonet, I. Ruiz-Trillo, Capsaspora owczarzaki. *Curr. Biol.* **27**, R829–R830 (2017).
28. H. Suga, I. Ruiz-Trillo, Development of ichthyosporeans sheds light on the origin of metazoan multicellularity. *Dev. Biol.* **377**, 284–292 (2013).
29. H. Suga, I. Ruiz-Trillo, in *Evolutionary Transitions to Multicellular Life: Principles and Mechanisms*, I. Ruiz-Trillo, A. M. Nedelcu, Eds. (Springer, 2015), vol. 2, pp. 117–128.
30. O. Dudin, A. Ondracka, X. Grau-Bové, A. A. B. Haraldsen, A. Toyoda, H. Suga, J. Bråte, I. Ruiz-Trillo, A unicellular relative of animals generates a layer of polarized cells by actomyosin-dependent cellularization. *eLife* **8**, e49801 (2019).
31. E. C. Raff, J. T. Villinski, F. R. Turner, P. C. J. Donoghue, R. A. Raff, Experimental taphonomy shows the feasibility of fossil embryos. *Proc. Natl. Acad. Sci. U.S.A.* **103**, 5846–5851 (2006).
32. J. A. Cunningham, K. Vargas, F. Marone, S. Bengtson, P. C. J. Donoghue, A multicellular organism with embedded cell clusters from the Ediacaran Weng'an biota (Doushantuo Formation, South China). *Evol. Dev.* **18**, 308–316 (2016).
33. Z. Yin, P. Liu, G. Li, P. Tafforeau, M. Zhu, Biological and taphonomic implications of Ediacaran fossil embryos undergoing cytokinesis. *Gondw. Res.* **25**, 1019–1026 (2014).
34. R. S. Sansom, S. E. Gabbott, M. A. Purnell, Non-random decay of chordate characters causes bias in fossil interpretation. *Nature* **463**, 797–800 (2010).
35. J. V. Bailey, S. B. Joye, K. M. Kalanetra, B. E. Flood, F. A. Corsetti, Evidence of giant sulphur bacteria in Neoproterozoic phosphorites. *Nature* **445**, 198–201 (2007).
36. N. J. Gostling, X. Dong, P. C. J. Donoghue, Ontogeny and taphonomy: An experimental taphonomy study of the development of the brine shrimp *Artemia salina*. *Palaeontology* **52**, 169–186 (2009).
37. E. N. U. Landon, P.-J. Liu, Z.-J. Yin, W.-C. Sun, X.-D. Shang, P. C. J. Donoghue, Cellular preservation of excysting developmental stages of new eukaryotes from the early Ediacaran Weng'an Biota. *Palaeoworld* **28**, 461–468 (2019).
38. P. A. Cohen, A. H. Knoll, R. B. Kodner, Large spinose microfossils in Ediacaran rocks as resting stages of early animals. *Proc. Natl. Acad. Sci. U.S.A.* **106**, 6519–6524 (2009).
39. Z. Yin, D. Zhao, B. Pan, F. Zhao, H. Zeng, G. Li, D. J. Bottjer, M. Zhu, Early Cambrian animal diapause embryos revealed by X-ray tomography. *Geology* **46**, 387–390 (2018).
40. R. Wood, A. G. Liu, F. Bowyer, P. R. Wilby, F. S. Dunn, C. G. Kenchington, J. F. H. Cuthill, E. G. Mitchell, A. Penny, Integrated records of environmental change and evolution challenge the Cambrian Explosion. *Nat. Ecol. Evol.* **3**, 528–538 (2019).
41. P. C. J. Donoghue, A. Kouchinsky, D. Waloszek, S. Bengtson, X.-P. Dong, A. K. Val'kov, J. A. Cunningham, J. E. Repetski, Fossilized embryos are widespread but the record is temporally and taxonomically biased. *Evol. Dev.* **8**, 232–238 (2006).
42. F. Marone, M. Stampanoni, Regridding reconstruction algorithm for real-time tomographic imaging. *J. Synchrotron Radiat.* **19**, 1029–1037 (2012).
43. Z. Yin, M. Zhu, New observations of the ornamented Doushantuo embryo fossils from the Ediacaran Weng'an Biota, South China. *Bull. Geosci.* **87**, 171–181 (2012).

Acknowledgments: We acknowledge provision of synchrotron radiation beamtime at the TOMCAT beamline X02DA of the Swiss Light Source, Paul Scherrer Institute, Villigen, Switzerland and the tomographic beamline BM5 of the European Synchrotron Radiation Facility, Grenoble, France. We also thank members of the Yin, Donoghue, and Bengtson laboratories for discussion and for assistance at the beamlines, along with beamline scientists F. Marone (TOMCAT, SLS) and P. Tafforeau (BM5, ESRF). **Funding:** This study was supported by the Strategic Priority Research Program (B) of the Chinese Academy of Sciences (XDB 26000000 and 18000000 to Z.Y., P.L., and M.Z.), the Natural Environment Research Council (NE/P013678/1 to P.C.J.D. and Z.Y.), the National Natural Science Foundation of China (41672013, 41661134048, and 41921002 to Z.Y., M.Z., P.C.J.D., and P.L.), and the Youth Innovation Promotion Association of the CAS (2017360 to Z.Y.). We also received funding from the European Union's Horizon 2020 research and innovation program under grant agreement no. 730872, project CALIPSOplus. **Author contributions:** Z.Y. and P.C.J.D. designed the study. Z.Y., P.L., and P.C.J.D. collected the fossils and data, which were analyzed by Z.Y., W.S., and P.C.J.D. All authors contributed to the interpretation of the results. P.C.J.D. and Z.Y. led the writing, to which all authors contributed. **Competing interests:** The authors declare that they have no competing interests. **Data and materials availability:** All the fossil specimens were deposited at NIGPAS. The supporting tomographic data are available from the University of Bristol Research Data Storage Facility (data.bris) at https://doi.org/10.5523/bris.tznl7b6dt7kr23cd1d5eokvcz. All data needed to evaluate the conclusions in the paper are present in the paper and/or the Supplementary Materials. Additional data related to this paper may be requested from the authors.

Submitted 24 January 2020
Accepted 21 April 2020
Published 12 June 2020
10.1126/sciadv.abb0083

Citation: Z. Yin, W. Sun, P. Liu, M. Zhu, P. C. J. Donoghue, Developmental biology of *Helicoforamina* reveals holozoan affinity, cryptic diversity, and adaptation to heterogeneous environments in the early Ediacaran Weng'an biota (Doushantuo Formation, South China). *Sci. Adv.* **6**, eabb0083 (2020).

Developmental biology of *Helicoforamina* reveals holozoan affinity, cryptic diversity, and adaptation to heterogeneous environments in the early Ediacaran Weng'an biota (Doushantuo Formation, South China)

Zongjun Yin, Weichen Sun, Pengju Liu, Maoyan Zhu and Philip C. J. Donoghue

Sci Adv **6** (24), eabb0083.
DOI: 10.1126/sciadv.abb0083